Inorganic Chemistry

Article

pubs.acs.org/IC

Electrogenerated Chemiluminescence from Heteroleptic Iridium(III) Complexes with Multicolor Emission

Yuyang Zhou,*[,†] Hongfang Gao,[‡] Xiaomei Wang,[†] and Honglan Qi*[,‡]

[†]Jiangsu Key Laboratory of Environmental Functional Materials, School of Chemistry, Biology and Material Engineering, Suzhou University of Science and Technology, Suzhou, Jiangsu 215009, P. R. China

[‡]Key Laboratory of Analytical Chemistry for Life Science of Shaanxi Province, School of Chemistry and Chemical Engineering, Shaanxi Normal University, Xi'an 710062, P. R. China

Supporting Information

ABSTRACT: Electrogenerated chemiluminescence (ECL) with different emission colors is important in the development of multichannel analytical techniques. In this report, five new heteroleptic iridium(III) complexes were synthesized, and their photophysical, electrochemical, and ECL properties were studied. Here, 2-(2,4-difluorophenyl)pyridine (dfppy, complex **1**), 2-phenylbenzo[d]thiazole (bt, complex **2**), and 2-phenylpyridine (ppy, complex **3**) were used as the main ligands to tune the emission color, while avobenzone (avo) was used as the ancillary ligand. For comparison, complexes **4** and **5** with 2-phenylpyridine and 2-phenylbenzo[d]thiazole as the main ligand, respectively, and acetyl acetone (acac) as the ancillary ligand were also synthesized. All five iridium(III) complexes had strong intraligand absorption bands ($\pi-\pi^*$) in the UV region (below 350 nm) and a featureless MLCT (d$-\pi^*$) transition in the visible 400−500 nm range. Multicolored emissions were observed for these five iridium(III) complexes, including green, orange, and red for complexes **4**, **5**, **2**, **1**, **3**, respectively. Density functional theory calculations indicate that the electronic density of the highest occupied molecular orbital is entirely located on the C^N ligands and the iridium atom, while the formation of the lowest unoccupied molecular orbital (LUMO) is complicated. The LUMO is mainly assigned to the ancillary ligand for complexes **1** and **3** but to the C^N ligand for complexes **2**, **4**, and **5**. Cyclic voltammetry studies showed that all these complexes have a reversible oxidation wave, but no reduction waves were found in the electrochemical windows of CH_2Cl_2. The $E^{ox}_{1/2}$ values of these complexes ranged from 0.642 to 0.978 V for complexes **3**, **4**, **2**, **5**, **1**, (in increasing order) and are all lower than that of $Ru(bpy)_3^{2+}$. Most importantly, when using tripropylamine as a coreactant, complexes **1**−**5** exhibited intense ECL signals with an emission wavelength centered at 616, 580, 663, 536, and 569 nm, respectively. In addition, complexes **1**, **2**, and **5** displayed approximately 2, 11, and 214 times higher ECL efficiencies than $Ru(bpy)_3^{2+}$ under identical conditions.

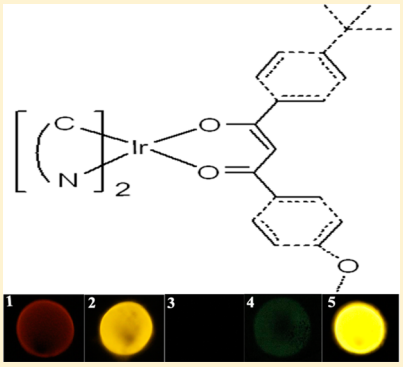

INTRODUCTION

Electrogenerated chemiluminescence (ECL) involves the generation of species at the surfaces of electrodes, which then undergo electron-transfer reactions to form light-emitting excited states, and has been developed to a commercially viable analytical technique.[1] Motivated by the demands of analytical applications, developing novel photoactive molecules with ECL has been an active research area. Since the first detailed ECL (or electrochemiluminescence) behavior of tri-2,2′-bipyridylruthenium(II) ($[Ru(bpy)_3]^{2+}$) was observed by Bard and co-workers in the early 1970s,[2,3] significant research efforts have been made to develop complexes of other metals in the recent few years, such as europium,[4] rhenium,[5] copper,[6] osmium,[7] aluminum,[8,9] terbium,[10] platinum,[11] iridium,[11−17] etc. Among the non-ruthenium systems studied so far, cyclometalated iridium(III) complexes are, in particular, becoming a major ECL subject because of their relatively long lifetimes, high photoluminescence (PL) efficiencies, and large Stokes shifts. Most importantly, unlike ruthenium(II) complexes with emissions centered approximately at 610 nm, iridium(III) complexes have the ability to span the emission range from the near-infrared[18] to deep blue[19] via ligand changing, which is useful in the development of multichannel analytical techniques.

In an early stage, a large number of iridium(III) complexes that were well-studied in organic light emitting diodes (OLEDs) have been developed directly as coreactant assisted ECL luminophores. For example, Richter and co-workers investigated the ECL properties of bis(3,5-difluoro-2-(2-pyridyl)phenyl-(2-carboxypyridyl))iridium(III) (FIrpic),[14] bis-[2,(2′-benzothienyl)-pyridinato-*N*,*C*3′](acetylacetonate Ir(III)) ($(btp)_2Ir(acac)$),[14] and *fac*-tris(2-phenylpyridine)iridium(III) ($Ir(ppy)_3$),[12] which were originally designed as dopants for OLEDs. Kapturkiewicz et al.[20] studied the substitute effect of iridium(III) complexes on the ECL properties. However, these efforts would not yield ideal results, and most of the ECL efficiencies are lower than that of $Ru(bpy)_3^{2+}$ although these

Received: October 6, 2014
Published: January 13, 2015

DOI: 10.1021/ic502444k
Inorg. Chem. 2015, 54, 1446−1453

iridium(III) complexes have outstanding PL properties. In 2005, Kim et al.[15] made a major breakthrough in the ECL studies of iridium(III) complexes. Two iridium complexes, namely, $(pq)_2Ir(acac)$ and $(pq)_2Ir(tmd)$ (pq = 2-phenylquinoline anion, acac = acetylacetonate anion, and tmd = 2,2′,6,6′-tetramethylhepta-3,5-dione anion), with much higher ECL efficiencies compared to that of $Ru(bpy)_3^{2+}$, have been successfully designed and synthesized. Subsequently, a large number of novel iridium(III) complexes have been deliberately designed and synthesized for ECL studies.[21−24] The relationships between the chemical structures and ECL properties of iridium(III) complexes have been gradually uncovered by further studies.[25−27]

Although the ECL studies of iridium(III) complexes are currently undergoing a great development, iridium(III) complexes with distinct ECL emission colors, which are very important in multichannel analytical applications, have rarely been deliberately designed or thoroughly studied so far.[28] As the emission color is usually closely related to the main ligand of the iridium(III) complexes, we chose 2-(2,4-difluorophenyl)-pyridine (dfppy), 2-phenylbenzo[d]thiazole (bt), and 2-phenylpyridine(ppy) (see Scheme 1) as the main ligands to tune the emission color as they are usually used to synthesize blue, orange, and green iridium(III) complexes, respectively. In addition to the main ligand, the ancillary ligand also has a strong influence on the photophysical properties, such as quantum efficiencies, of iridium(III) complexes.[29] Acetyl acetone (acac, see Scheme 1), a well-known ancillary ligand in iridium(III) complexes, has been largely studied.[15,30,31] However, its derivative, avobenzone (avo, see Scheme 1), which was originally used as the main ingredient in sunscreen products due to its strong absorption in the 320−400 nm range, has never been used as the ancillary ligand of iridium(III) complexes so far. Taking into account that difluoroboron complexes with the avobenzone ligand have been recently reported to have unique mechanochromic properties,[32,33] we are curious about their roles in iridium(III) complexes. Therefore, three iridium(III) complexes with an avobenzone ligand (see **1**, **2**, and **3** in Scheme 2) and two comparative iridium(III) complexes with an acac ligand (see **4** and **5** in Scheme 2) were designed and successfully synthesized in this work. Furthermore, their photophysical properties, especially the ECL properties, were thoroughly studied in this work.

Scheme 1. Chemical Structures of the Coordination Ligands Used in This Work

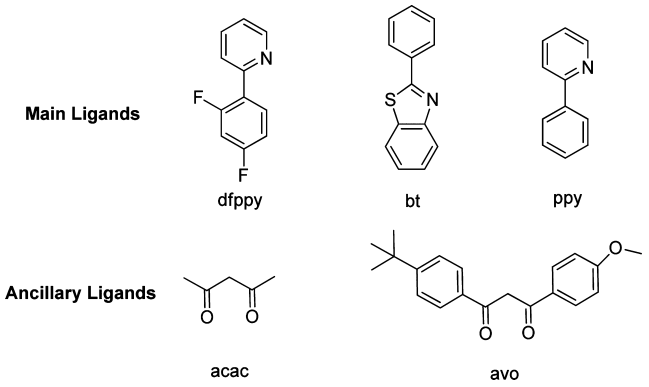

RESULTS AND DISCUSSION

Absorption and Photoluminescence. The electronic absorption spectra of **1**−**5** in a dichloromethane solution are presented in Figure 1A. Similarly to other previously reported heteroleptic iridium(III) complexes,[34−40] all the iridium(III) complexes in this work have strong intraligand absorption bands ($\pi-\pi^*$) in the UV region (below 350 nm) and a featureless MLCT ($d-\pi^*$) transition in the visible range of 400−500 nm (ε < 8000 M^{-1} cm^{-1}). According to Figure 1A, the effect of avo on the absorption spectra lies mainly in the intraligand absorption bands. Note that complexes **2** and **3**, with the avo ligand, have much stronger intraligand absorption bands ($\pi-\pi^*$) than the corresponding complexes **5** and **4**, with an acac ligand. This is reasonably explained by the avo ligand having a larger degree of conjugation than the acac ligand.

The normalized emission spectra of **1**−**5** are shown in Figure 1B. Although complexes **1**−**3** all have an ancillary avo ligand, they displayed a great variation in their emission spectra. According to previously reported studies,[30,41] the luminescence of iridium(III) complexes is related to the energies of the main (C^N) and ancillary ligands. When the energy of the main ligand (C^N) is lower than that of the ancillary ligand, the luminescence is dominated by the C^N ligand and the metal−ligand charge-transfer (MLCT) state. However, if the triplet energy of the ancillary ligand is lower than that of the main ligand or the ^{3}MLCT state, the transition channel from "$(C^N)_2Ir$" or ^{3}MLCT to the triplet state of the ancillary ligand would be open, and the luminescence would finally be dominated by the triplet state of the ancillary ligand. For complexes **1** and **3**, the triplet energy level of avo is lower than that of the C^N ligand and the MLCT state; therefore, the emission mainly originated from the triplet state of the ancillary ligand and was weak. However, the triplet energy of the ancillary ligand of complexes **2**, **4**, and **5** is higher than the energy of the corresponding C^N ligand and MLCT state, and the complexes have an efficient emission from the excited state

Scheme 2. Chemical Structures of the Iridium(III) Complexes $(C^N)_2Ir(O^O)$ Used in This Work

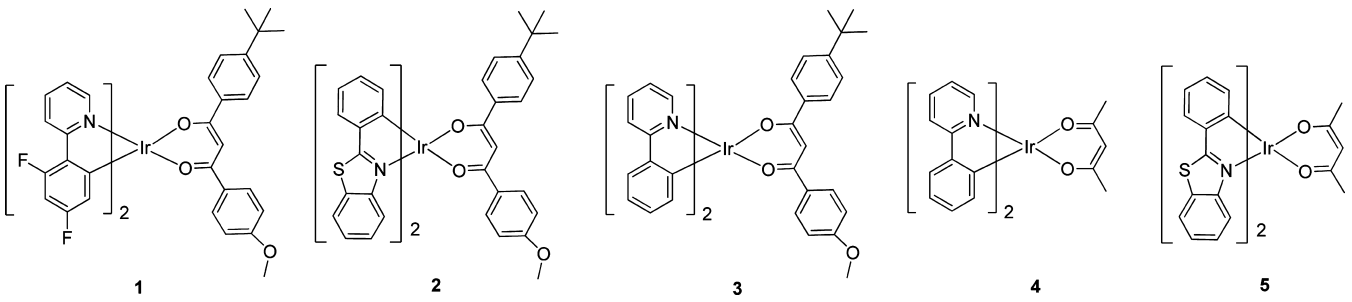

DOI: 10.1021/ic502444k
Inorg. Chem. 2015, 54, 1446−1453

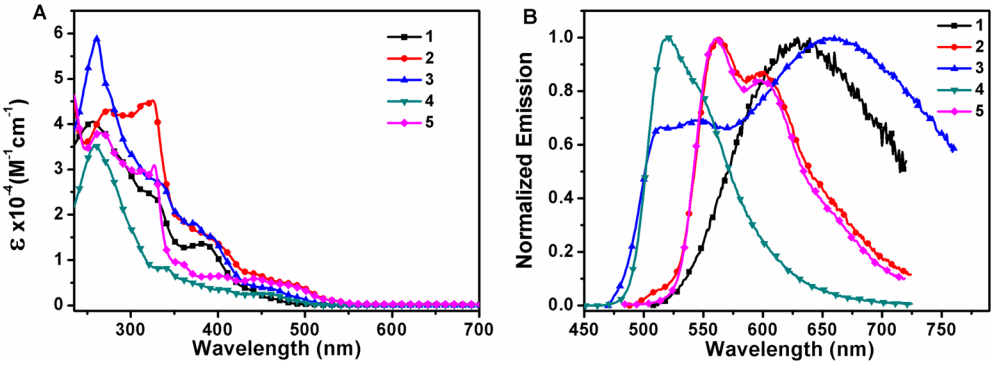

Figure 1. Absorption (A) and normalized emission (B) spectra of **1**−**5** (40 μM) in deaerated dichloromethane solution. ε is the molar extinction coefficient.

of the $(C^N)_2Ir$ fragment. The maximum emission wavelength is 629, 563, 664, 519, and 562 nm, respectively, for complex **1** to complex **5**. The presence of two fluoride atoms on the main ligand of complex **1** induced a blue shift of approximately 35 nm in the emission wavelength, compared to that of complex **3**. The emission of complex **4** was dominated by the energies of the C^N ligand or MLCT state and had a hypsochromic shift, compared to complex **3** whose emission was dominated by the energies of the triplet state of the ancillary ligand. However, complexes **2** and **5** have the same emission wavelength because they have the same C^N main ligand, and their emission both originate from the excited state of $(C^N)_2Ir$ fragment.

Note that complex **3** has multiple emission peaks, as shown in Figure 1B. In addition to the main emission at 664 nm from the transition of the triplet state of ancillary ligand, there are also emission peaks between 510 and 540 nm, which are similar to those of complex **4**. Because complex **4** has the same C^N ligand as complex **3**, we reasonably explained the emission of complex **3** at shorter wavelengths (510−540 nm) as ascribed to the excited state of the $(C^N)_2Ir$ fragment. The following theoretical studies of electron localization on frontier orbitals provide a better explanation.

To measure the PL quantum efficiency (Φ_{PL}), we chose *fac*-$Ir(ppy)_3$ as a reference, under an excitation light of 360 nm. This selected wavelength is a compromise that enabled both the iridium(III) luminophores and *fac*-$Ir(ppy)_3$ to be compared under the condition that all the compounds have similar absorptions. On the basis of the excitation coefficients at 360 nm and the emission intensities, the Φ_{PL} values of these iridium(III) complexes were calculated by using *fac*-$Ir(ppy)_3$ as the standard (0.40, in dichloromethane[42]). The relative quantum efficiencies of complexes **1**−**5** are listed in Table 1. These five complexes have a great variation in Φ_{PL}. Unfortunately, complexes **3** and **2** with the avo ligand have a lower Φ_{PL} value than that of complexes **4** and **5** with the acac ligand. This may be caused by the presence of much more nonradiative transition channels in the avo ligand with *t*-butyl and methoxyl groups. Furthermore, complexes **2**, **4**, and **5** exhibited higher Φ_{PL} than complexes **1** and **3** because their emissions arise from the excited state of $(C^N)_2Ir$ or ^{3}MLCT, which are much more efficient than the transition from the triplet state of the ancillary ligand.[30]

The emission lifetimes of **1**−**5** in degassed CH_2Cl_2 at room temperature were also tested and are listed in Table 1. Complexes **1**, **2**, and **3**, with the avo ligand, all have a longer lifetime than complexes **4** and **5** with the acac ligand, contrary to the negative effect of the avo ligand on Φ_{PL}.

Table 1. Spectroscopic Data of 1−5 in Dichloromethane Solution

	absorption	emission		
complex	λ (nm) [$\varepsilon \times 10^{-4}$ ($M^{-1}cm^{-1}$)]	λ_{max} (nm)	Φ_{PL}[a]	lifetime τ_P (μs) at room temperature
1	249[3.17], 256 [4.02], 386 [1.33]	629	0.014	2.38
2	275 [4.30], 314 [4.45], 325 [4.50], 381 [1.60], 440 [0.72], 480 [0.48]	563, 599	0.025	2.41
3	260 [5.86], 326 [2.80], 372 [1.82], 394 [1.93], 456 [0.41]	513, 546, 664	0.017	2.78
4	359 [3.52], 337 [0.85], 403 [0.34], 456 [0.24]	519	0.112	2.35
5	265 [3.79], 312 [2.99], 326 [3.08] 355 [0.97], 400 [0.67], 442 [0.58]	562, 597	0.224	2.01

[a]The reference is *fac*-$Ir(ppy)_3$ (Φ_{PL} is 0.40), in deaerated CH_2Cl_2.

Theoretical Calculations. To further investigate the properties of $(C^N)_2Ir(O^O)$ in this work, we used density functional theory (DFT)[43] with B3LYP[44−46] to calculate the highest occupied molecular orbital/lowest unoccupied molecular orbital (HOMO/LUMO) energy levels and the electronic ground states of **1**−**5**. The 6-31G basis set[47] was used for C, N, H, O, and the LANL2DZ basis set[48,49] was employed for the iridium atom; these sets have been shown to be reliable for theoretical studies of cyclometalated iridium(III) complexes.[50−52]

As Figure 2 shows, the electronic density of the HOMO of complexes **1** and **3** was localized on the C^N ligands and the iridium atom, while the LUMO was mainly assigned to the ancillary ligand. This result indicated that the excited state of the avo ligand played important role in the emission of **1** and **3**. As for the multiple emission peaks of complex **3**, a reasonable explanation could be found after careful investigation of the electronic distribution. According to Figure 2, beside the intense electronic contribution of the avo ligand to the LUMO, there is also some electron density from the phenyl group of the C^N ligand in the LUMO. Therefore, the emission of complex **3** is related to both the triplet state of avo and the excited state of the C^N main ligand. The complicated excited states of complex **3** induced the multiple emission peaks. The emission of complex **3** at shorter wavelengths, in Figure 1B, originated from the state of the C^N main ligand, and the emission at longer wavelengths should arise from the state of

DOI: 10.1021/ic502444k
Inorg. Chem. 2015, 54, 1446−1453

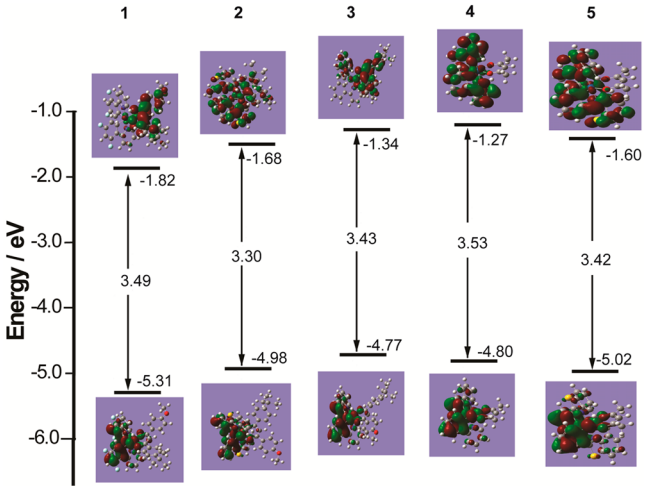

Figure 2. Contour plots of HOMO and LUMO of **1**−**5** used in this work.

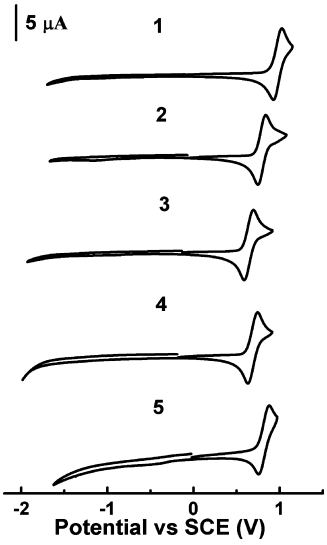

Figure 3. Cyclic voltammograms of 1 mM **1**−**5** in CH_2Cl_2 solutions containing 0.1 M $TBAPF_6$. Scan rate: 0.1 V/s, Pt electrode surface area: 0.029 cm^2.

the avo ligand. For complexes **2**, **4**, and **5**, both the HOMO and LUMO are assigned to a mixture of the main ligand and the iridium atom, the ancillary ligands having very little electronic contribution to the LUMO. Therefore, the emissions of complexes **2**, **4**, and **5** are mainly dominated by the state of $(C^N)_2Ir$ or MLCT. In conclusion, the theoretical results in this work provide a better explanation of the emission, which is in line with the former reported literature.[30]

In addition, complex **1** possesses two electron-withdrawing F atoms on the main ligand, which are not present in complex **3**. The energy gap (ΔE) between the HOMO and LUMO is also calculated and shown in Figure 2. The fluorine atoms induced the increase in ΔE from 3.43 eV for complex **3** to 3.49 eV for complex **1**, which reasonably explained the hypsochromic shift from complex **3** to complex **1** observed in the PL characterization experiment (see Figure 1B). The differences in the ancillary ligand between complexes **2** and **5** have very little effect on the HOMO and LUMO energy levels because their main ligand is the same.

Electrochemistry and Electrogenerated Chemiluminescence. As the redox parameters are critical to ECL, the cyclic voltammograms (CVs) of **1**−**5** were characterized in this work. All electrochemical measurements were carried out in a CH_2Cl_2 solution with 0.1 M tetra-*n*-butylammonium hexafluorophosphate ($TBAPF_6$) as the supporting electrolyte. As shown in Figure 3, the CV of **1**−**5** at a scan rate of 0.1 V/s showed a reversible one-electron oxidation with a half-wave potential, $E_{1/2}$, of +0.978, +0.795, +0.642, +0.683, +0.845 V versus saturated calomel electrode (SCE), respectively. The oxidative wave is assigned to the $(C^N)_2Ir(O^O)^0/(C^N)_2Ir(O^O)^+$ couple.[20,42] Complexes **1**−**5** exhibit a lower oxidation potential compared to $Ru(bpy)_3^{2+}$.[53] No reduction peak was observed until ca. −2.0 V versus SCE in this solvent. Tetrahydrofuran (THF), which has a more negative working potential range, was chosen as solvent to study the reduction of these compounds. Complexes **1**, **2**, **3**, and **5** gave irreversible reduction peaks at potentials more negative than −2.0 V, but **4** did not show any reduction peaks, even at potentials more negative than −2.8 V versus SCE (Figure S1 in the Supporting Information).

The $E_{1/2}$ of these five compounds varied slightly due to the differences in their chemical structure and is ordered as follows:**1** > **5** > **2** > **4** > **3**. Complex **3** is more easily oxidized and reduced than the other complexes. Despite the discrepancies between the theoretical data (see Figure 2) and the electrochemistry-based data (see Table 2), the general trend of the theoretical HOMO energies is in line with that of the experimental values, and both series of energies follow the sequence **1** < **5** < **2** < **4** < **3**.

Table 2. Summarized Data of Electrochemical and ECL Properties of Complexes 1−5 Used in This Work

complex	$E_{1/2}^{ox}$ (vs SCE, V)[a]	E_p^{red} (vs SCE, V)[b]	HOMO[c]	λ_{max} of ECL emission (nm)	Φ_{ECL}[d]
1	+0.978	−2.330	−5.378	616	2
2	+0.795	−2.361	−5.195	580	11
3	+0.642	−2.362	−5.042	663	0.03
4	+0.683		−5.083	536	0.96
5	+0.845	−2.288	−5.245	569, 603	214

[a]In CH_2Cl_2 solution. [b]In THF solution. [c]HOMO = $-(4.4 + E_{1/2}^{ox})$. [d]Relative to $[Ru(bpy)_3]^{2+}$ defined as 1 in this work.

As no negative reductive waves of $(C^N)_2Ir(O^O)$ were found in the electrochemical window of CH_2Cl_2, an annihilation of the ECL could not be generated in this solvent. In combination with the redox properties of **1**−**5** from the CV experiments, here, coreactant ECL tied to the oxidation was possible, and the ECL behaviors of **1**−**5** in the presence of TPA as a coreactant were studied. The results of an ECL experiment with complexes **1**−**5** and 10 mM TPA in CH_2Cl_2 containing 0.1 M $TBAPF_6$ at a Pt electrode are shown in Figure 4. A strong ECL signal appeared at the oxidation potential of five complexes **1**−**5**. No ECL was seen upon oxidation when either the iridium(III) complex or TPA was absent from the test solution. The addition of TPA caused the oxidation current of complexes **2**−**5** to increase sharply, while the reversible peak disappeared, as expected of a catalytic reaction wave.[54] Interestingly, for complex **1**, two irreversible oxidation peaks ascribed to TPA and complex **1** were observed in the ECL-generated solution because of the more positive oxidation potential of complex **1**.

DOI: 10.1021/ic502444k
Inorg. Chem. 2015, 54, 1446−1453

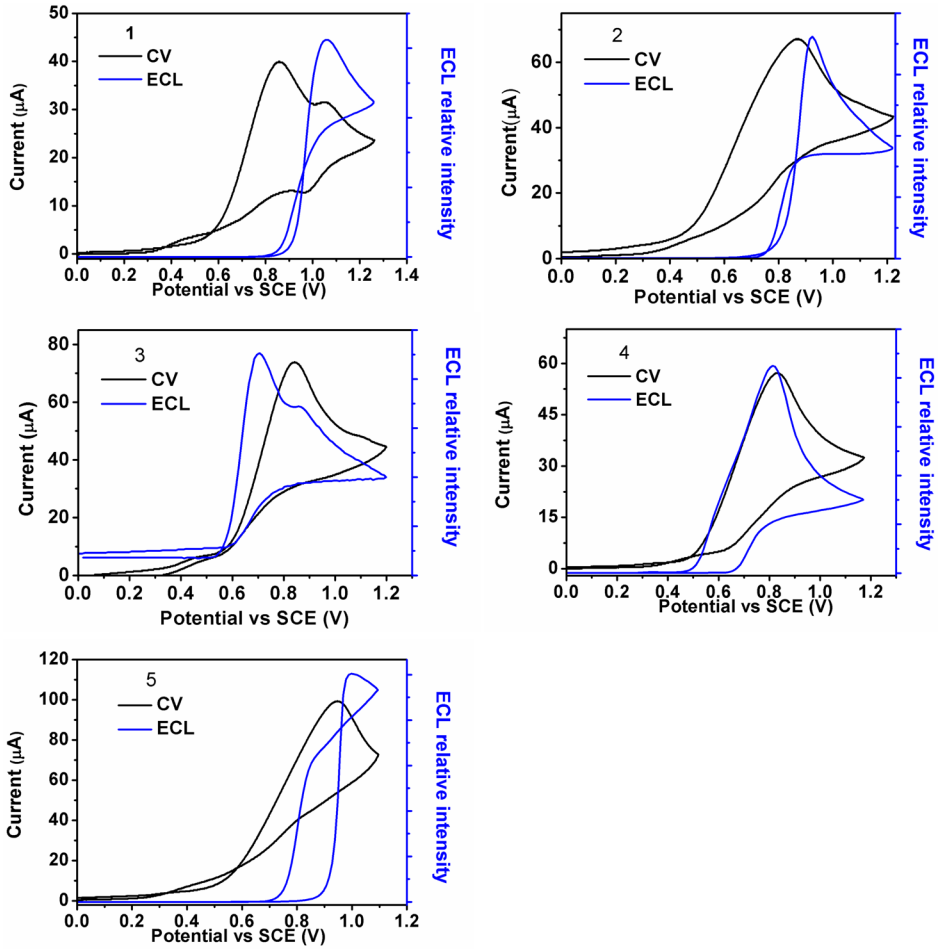

Figure 4. CV and ECL intensity over the potential plots of 1 mM complexes **1**−**5** in CH_2Cl_2 solution containing 0.1 M $TBAPF_6$ and 10 mM TPA. Scan rate: 0.1 V/s.

Figure 5 shows the ECL spectra of complexes **1**−**5** obtained by pulsing between 0 and the oxidation potential (80 mV past the oxidation potential). The physical and spectral data for the coreactant ECL are listed in Table 2. As shown in Figure 5B, four compounds produced green, orange, and red ECL emissions that were visible to the naked eyes in a dark room (photographs taken with Canon camera 770D EOS), except for complex **3**, which has a low ECL efficiency. The maximum ECL emission of $(C^N)_2Ir(O^O)$ was very close to the PL emission, indicating that they originate from the same excited states. The difference between the ECL and the PL spectra can be ascribed to the different solutions (the ECL solution contained a coreactant) and slit widths used in the experiments. The red shift observed in the ECL emission peaks proceeding from **4**, **5**, **2**, **1**, and **3** is consistent with the PL spectra. The ECL efficiencies (Φ_{ECL}) were also calculated according to the equation $\Phi_{ecl,s} = \Phi_{ecl,ref}*(I_s/I_{ref})$, in which $\Phi_{ecl,s}$ demonstrates the ECL efficiency of the iridium complex, $\Phi_{ecl,ref}$ demonstrates the ECL efficiency of $Ru(bpy)_3^{2+}$ defined as 1 in this work, I_s is the number of integrations of the ECL signals of the iridium complexes, and I_{ref} is the number of integrations of the ECL signals of the reference generated under the same condition. The data are listed in Table 2. The Φ_{ECL} values followed the sequence **3** < **4** < **1** < **2** < **5**. Note that complexes **1**, **2**, and **5** exhibit much stronger ECL emission than the widely used $Ru(bpy)_3^{2+}$ under identical conditions, which also can be visibly seen from the ECL emission photo under identical conditions (Figure S2 in the Supporting Information).

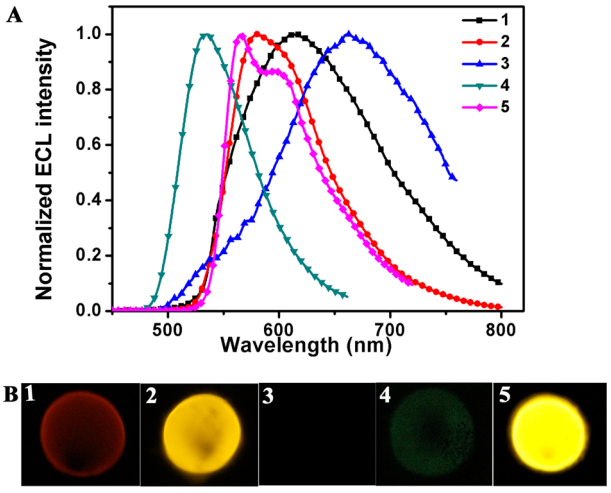

Figure 5. Normalized ECL spectra (A) and ECL emission photographs (B) of 1 mM complexes **1**−**5** in CH_2Cl_2 solution containing 10 mM TPA and 0.1 M $TBAPF_6$. Potential pulsing from 0 to 80 mV over the peak potential of the corresponding iridium(III) complexes.

On the basis of the understanding of the oxidative−reduction mechanism that led to the ECL of the $Ru(bpy)_3^{2+}$/TPA

DOI: 10.1021/ic502444k
Inorg. Chem. 2015, 54, 1446−1453

system[55,56] and other iridium complex/TPA systems,[23,57] we proposed that the present $(C^N)_2Ir(O^O)$/TPA system followed the same mechanism, depicted in Scheme 3. The

Scheme 3. ECL Generation Mechanism for Iridium(III) Complexes $(C^N)_2Ir(O^O)$

$$(C^N)_2Ir(O^O) \longrightarrow (C^N)_2Ir(O^O)^+ + e^- \quad (1)$$

$$N(C_3H_7)_3 \longrightarrow N(C_3H_7)_3^{\bullet+} + e^- \quad (2)$$

$$N(C_3H_7)_3^{\bullet+} \longrightarrow CH_3CH_2CHN(C_3H_7)_2^{\bullet} + H^+ \quad (3)$$

$$CH_3CH_2CHN(C_3H_7)_2^{\bullet} + (C^N)_2Ir(O^O)^+ \longrightarrow (C^N)_2Ir(O^O)^* + \text{products} \quad (4)$$

$$(C^N)_2Ir(O^O)^* \longrightarrow (C^N)_2Ir(O^O) + h\upsilon \quad (5)$$

generation of $(C^N)_2Ir(O^O)^+$ (eq (1)) and $TPA^{\bullet+}$ radical cation (eq (2)) are two electrochemical processes followed by two chemical processes (eqs (3) and (4)), and a photon generation physical process (eq (5)). Given that all the iridium(III) complexes show a good reversibility of the oxidative wave, we can ignore the effect of the stability of $(C^N)_2Ir(O^O)^+$ on the value of Φ_{ECL}.[22] According to previous studies,[26,27] the energy level of the LUMO is closely related to the efficiency of eq (4); the lower the LUMO of $(C^N)_2Ir(O^O)$, the more efficient the process involved in eq (4), and the higher the Φ_{ECL}. In this work, the energy of the LUMO obtained from theoretical calculations follows the order **1** < **2** < **5** < **3** < **4**; however, the Φ_{ECL} followed the sequence **5** > **2** > **1** > **4** > **3**. The discrepancy indicated that the ECL process is much more complicated, and the Φ_{ECL} is hardly a function of a single parameter.

CONCLUSION

In this work, dfppy, bt, and ppy were deliberately selected to control the emission of heteroleptic iridium(III) complexes, and avobenzone (avo) was used for the first time as a novel ancillary ligand to construct iridium(III) complexes. Three iridium(III) complexes with avo ligand and two comparative complexes with acac ligand have been successfully designed, synthesized, and characterized. All these iridium(III) complexes, $(C^N)_2Ir(O^O)$, have a reversible oxidative peak at a lower potential compared to $Ru(bpy)_3^{2+}$. Under the assistance of TPA, these iridium(III) complexes displayed intense ECL signals and have different ECL emission colors. Three iridium(III) complexes (i.e., **1**, **2**, and **5**), with extremely higher ECL efficiency than $Ru(bpy)_3^{2+}$ when using TPA as a coreactant,were reported in this work for the first time. Given the different ECL colors and intense ECL signals, these results would be very useful in the development of multichannel analytical techniques.

EXPERIMENTAL SECTION

Chemicals. 2-(2,4-Difluorophenyl)pyridine (dfppy), 2-phenylbenzothiazole (bt), 2-phenylpyridine (ppy), avobenzone (avo), and acetyl acetone (acac) were all purchased from J&K Chemical Ltd., and 2-ethoxyethanol was purchased from Sinopharm Chemical Reagent Co. Ltd. Dichloromethane (DCM, 99.8%) was obtained from Sigma-Aldrich (St. Louis, MO) and transferred directly into an argon-atmosphere glovebox (MBraun Inc., Stratham, NH) without further purification. Electrochemical-grade $TBAPF_6$ was dried in a vacuum oven at 100 °C and then transferred directly into an argon-atmosphere glovebox.

Synthesis and Characterization. The dichlorobridged iridium dimer is the critical precursor to synthesize **1**−**5** in this work, and its synthesis route was demonstrated in Scheme 4. A solution of $IrCl_3 \cdot 3H_2O$ (1 equiv) and C^N ligand (2 equiv) in a mixture of 2-ethoxyethanol/H_2O (3:1 v/v) was refluxed under argon atmosphere for 24 h. After it cooled to room temperature, the solution was filtered, and the precipitate was successively washed with water, ethanol, and *n*-hexane. The dichlorobridged iridium dimer was obtained after drying.

Scheme 4. Synthesis Route of Dichlorobridged Dimer Used in This Work

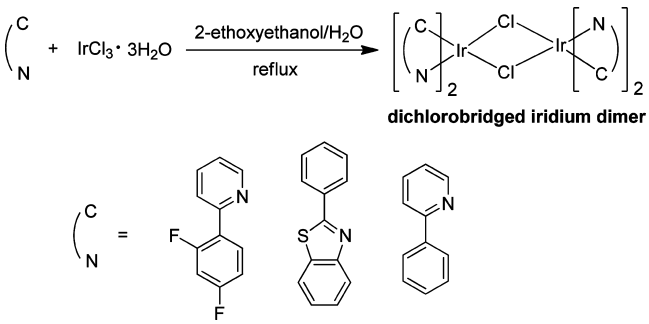

The dichlorobridged iridium dimer was used without further purification to synthesize complexes **1**−**5** in this work. For complex **1**, **2**, and **3**, a solution of 2.2 equiv of avo ligand, 1 equiv of corresponding dichlorobridged iridium(III) dimer (dfppy for complex **1**, bt for complex **2**, and ppy for complex **3**), and 22 equiv of Na_2CO_3 in 2-ethoxyethanol was refluxed for 24 h. The solvent was rotoevaporated, and the residue was chromatographed on a silica gel column with a CH_2Cl_2/*n*-hexane (various ratios based on the properties of the compounds) eluent to give the pure product. Complexes **4** and **5** were also successfully synthesized by replacing the avo ligand by acac ligand on the basis of synthesizing complex **3** and complex **2**, respectively.

Caution! *Use protective gloves with proper protection and carefully handle solvents for all processes being performed.*

Complex **1** (Yield: 69%).^{1}H NMR ($CDCl_3$, 400 MHz). δ ppm: 1.29 (s, 9 H), 3.81 (s, 3 H), 5.77 (m, 2 H), 6.38 (m, 2 H), 6.52 (d, J = 8 Hz, 2 H), 6.56 (s, 1 H), 7.07 (m, 2 H), 7.35 (d, J = 4 Hz, 2 H), 7.77 (m, 6 H), 8.24 (d, J = 8 Hz, 2 H), 8.53 (m, 2 H). ^{13}C NMR ($CDCl_3$, 100 MHz). δ ppm: 31.11, 34.85, 55.36, 93.88, 97.05,113.52, 115.22, 121.60, 122.56, 125.26, 126.64, 128.68, 133.21, 137.80, 148.01, 148.04, 152.02, 152.09, 152.29, 153.86, 159.40, 159.53, 161.24, 161.58, 161.97, 162.10, 163.78, 163.90, 165.25, 165.32, 178.24, 178.58. ^{19}F NMR ($CDCl_3$, 376 MHz). δ ppm: −111.45 (m), −109.38 (q, J = 9.02 Hz). Time-of-flight (TOF) mass spectral data: calculated $[M + H]^+$ 883.2129, observed $[M + H]^+$ 883.2160.

Complex **2** (Yield: 81%). ^{1}H NMR ($CDCl_3$, 400 MHz). δ ppm: 1.28 (s, 9 H), 3.79 (s, 3 H), 6.41 (s, 1 H), 6.52 (m, 2 H), 6.68 (m, 2 H), 6.79 (m, 2 H), 6.90 (m, 2 H), 7.19 (m, 2 H), 7.31 (m, 4 H), 7.80 (m, 6 H), 7.90 (m, 2 H), 8.10 (m, 2 H). ^{13}C NMR ($CDCl_3$, 100 MHz). δ ppm: 31.12, 34.76, 55.29, 94.91, 113.31, 120.31,120.39, 120.89, 120.93,122.06,124.89, 125.03, 125.60, 126.59, 127.28, 127.41, 128.62, 129.81,131.12, 131.15, 133.45, 135.21,135.28, 138.41, 141.93, 141.96, 148.95, 149.08, 150.77,150.86, 153.13, 161.13, 179.09, 179.64, 180.13, 180.16. TOF mass spectral data: calculated $[M + H]^+$ 923.1948, observed $[M + H]^+$ 923.1985.

Complex **3** (Yield: 69%).^{1}H NMR ($CDCl_3$, 400 MHz). δ ppm: 1.27 (s, 9 H), 3.78 (s, 3 H), 6.36 (t, J = 7.6 Hz, 2 H), 6.53 (s, 1 H), 6.72 (m, 2 H), 6.78 (m, 2 H), 6.84 (m, 2 H), 7.00 (m, 2 H), 7.31 (d, J = 7.6 Hz, 2 H), 7.57 (m, 2 H), 7.63 (m, 2 H), 7.79 (m, 6 H), 8.59 (dd, J = 6,10 Hz, 2 H). ^{13}C NMR ($CDCl_3$, 100 MHz). δ ppm: 31.12, 34.78, 55.32,93.71, 113.35, 118.18, 118.19, 120.37, 120.39, 121.32, 121.34, 123.60, 125.09, 126.64, 128.63, 128.77, 133.21, 133.26, 133.86, 136.71, 136.73, 138.73, 144.87, 144.91, 148.14, 148.18, 148.28, 148.49, 153.32,

DOI: 10.1021/ic502444k
Inorg. Chem. 2015, 54, 1446−1453

161.21, 168.61, 177.90, 178.26. TOF mass spectral data: calculated $[M + H]^+$ 811.2506, observed $[M + H]^+$ 811.2527.

Complex **4** (Yield: 82%). ^{1}H NMR ($CDCl_3$, 400 MHz). δ ppm:1.78 (s, 6 H), 5.21 (s, 1 H), 6.26 (m, 2 H), 6.68 (m, 2 H), 6.78 (m, 2 H), 7.13 (m, 2 H), 7.55 (dd, J = 6.4, 1.6 Hz, 2 H), 7.72 (m, 2 H), 7.84 (m, 2 H), 8.52 (m, 2 H). ^{13}C NMR (deuterated dimethyl sulfoxide (DMSO-d_6), 100 MHz). δ ppm: 28.67, 100.74, 119.29, 120.74, 122.89, 124.39, 128.76, 133.02, 138.33, 145.50, 147.82, 148.18, 167.97, 184.38. TOF mass spectral data: calculated $[M + H]^+$ 601.1462, observed $[M + H]^+$ 601.1481.

Complex **5** (Yield: 85%). ^{1}H NMR (DMSO-d_6, 400 MHz). δ ppm: 1.72(s, 6 H), 5.20 (s, 1 H), 6.22 (m, 2 H), 6.60 (td, J = 7.6, 1.2 Hz, 2 H), 6.85 (td, J = 7.2, 0.8 Hz, 2 H), 7.56 (m, 4 H), 7.74 (m, 2 H), 7.94 (m, 2 H), 8.25 (m, 2 H). ^{13}C NMR (DMSO-d_6, 100 MHz). δ ppm: 28.43, 101.96, 119.66, 121.57, 124.07, 126.05, 126.38, 128.17, 130.27, 131.43, 134.85, 142.03, 148.46, 150.52, 180.42, 185.79. TOF mass spectral data: calculated $[M + H]^+$ 711.0880, observed $[M + H]^+$ 711.0867.

Apparatus and Methods. ^{1}H NMR, ^{13}C NMR, and ^{19}F NMR spectra were acquired on a VARIAN 400 MHz magnetic resonance spectrophotometer. The solvent signals were used for ^{1}H NMR ($\delta(CDCl_3)$ = 7.26 ppm and δ(DMSO-d_6) = 2.50 ppm) and ^{13}C NMR ($\delta(CDCl_3)$ = 77.0 ppm and δ(DMSO-d_6) = 39.5 ppm) as the internal standard, while the signal of C_6F_6 ($\delta(C_6F_6)$ = −162.90 ppm) was used as external standard for ^{19}F NMR spectra. Mass spectra were measured on a Varian ProStar LC240 (America). UV−vis absorption spectra were recorded using a 1 cm quartz cuvette on UV−vis spectrophotometer (UV-2450, Shimadzu Corporation, Japan). Fluorescence spectra were recorded by using a Edinburgh FLS920 type steady-state/transient spectrometer. UV−vis absorbance and fluorescence measurements were carried out in deaerated CH_2Cl_2 solution.

Dichloromethane was used as the solvent, and 0.1 M $TBAPF_6$ was used as the supporting electrolyte for all electrochemical investigations. All electrochemical experiments were performed under anhydrous conditions. For measurements made outside of the glovebox, the electrochemical cell was assembled inside the glovebox and sealed with a Teflon cap with a rubber O-ring. Stainless steel rods driven through the cap formed the electrode connections. Electrochemical experiments were performed using a three-electrode setup with a Pt disk working electrode (2.0 mm diameter), a Pt auxiliary electrode, and a quasi-reference silver wire electrode. The area of the Pt disk electrode was 0.029 cm^2. The working electrode was polished after each experiment with 0.3 μm alumina (Buehler, Ltd., Lake Bluff, IL) for several minutes, sonicated in water and in ethanol for 5 min each, and dried in an oven at 120 °C. CV potentials were calibrated with ferrocene as a standard, taking E^0 = 0.342 V versus SCE. CV measurements were carried out with a CHI 660 electrochemical workstation (Chenhua Instruments Co., Shanghai, China). The ECL transients and simultaneous CV and ECL measurements were recorded using a MPI-A ECL detector (Xi'an Remax Electronics, China).

ECL spectra were generated by pulsing from 0 to 80 mV past the oxidation peak of the iridium(III) complexes with a step time of 0.1 s using TPA as a coreactant. ECL spectra were generated using CHI 440 and collected with the Cary Eclipse fluorescence spectrophotometer. The emission slits were set to 20 nm bandwidth.

Theoretical Calculations. The ground states of the iridium(III) complexes were all optimized by using DFT.[43] All the DFT calculations were carried out with the Gaussian 03 software package,[58] and B3LYP[44−46] was adopted here. The 6-31G basis set[47] was employed for C, N, H, and O, and the LANL2DZ basis set[48] was used for the iridium atom,[49] which has proved reliable for cyclometalated iridium(III) complexes.[50−52]

■ ASSOCIATED CONTENT

Ⓢ Supporting Information

Cyclic voltammograms of complexes **1**−**5** in THF solution; normalized ECL spectrum of 1 mM $Ru(bpy)_3^{2+}$ in CH_2Cl_2 solution containing 10 mM TPA and 0.1 M $TBAPF_6$; ^{1}H NMR, ^{13}C NMR, and TOF mass spectra of complexes **1**−**5**; ^{19}F NMR of complex **1**; Cartesian coordinates in *xyz* format of the optimized geometries of complexes **1**−**5**. This material is available free of charge via the Internet at http://pubs.acs.org.

■ AUTHOR INFORMATION

Corresponding Authors

*E-mail: zhouyuyang@mail.usts.edu.cn. (Y. Zhou)

*E-mail: honglanqi@snnu.edu.cn. (H. Qi)

Funding

The Opening Project (No. SJHG1305) of the Jiangsu Key Laboratory for Environment Functional Materials; Science Foundation of Suzhou University of Science and Technology (No. XKQ201419); Excellent Innovation Team in Science and Technology of University in Jiangsu Province; The National Science Foundation of China (No. 21375084); The Natural Science Basic Research Plan in Shaanxi Province of China (No. 2013KJXX-73); Collaborative Innovation Center of Technology and Material of Water Treatment.

Notes

The authors declare no competing financial interest.

■ ACKNOWLEDGMENTS

The authors are grateful to the Opening Project (No. SJHG1305) of the Jiangsu Key Laboratory for Environment Functional Materials, Science Foundation of Suzhou University of Science and Technology (No. XKQ201419), Excellent Innovation Team in Science and Technology of University in Jiangsu Province, the National Science Foundation of China (No. 21375084), the Natural Science Basic Research Plan in Shaanxi Province of China (No. 2013KJXX-73), and Collaborative Innovation Center of Technology and Material of Water Treatment for financial supports.

■ REFERENCES

(1) Miao, W. *Chem. Rev.* **2008**, *108*, 2506−2553.

(2) Tokel-Takvoryan, N. E.; Hemingway, R. E.; Bard, A. J. *J. Am. Chem. Soc.* **1973**, *95*, 6582−6589.

(3) Tokel, N. E.; Bard, A. J. *J. Am. Chem. Soc.* **1972**, *94*, 2862−2863.

(4) Richter, M. M.; Bard, A. J. *Anal. Chem.* **1996**, *68*, 2641−2650.

(5) Richter, M. M.; Debad, J. D.; Striplin, D. R.; Crosby, G. A.; Bard, A. J. *Anal. Chem.* **1996**, *68*, 4370−4376.

(6) McCall, J.; Bruce, D.; Workman, S.; Cole, C.; Richter, M. M. *Anal. Chem.* **2001**, *73*, 4617−4620.

(7) Bruce, D.; Richter, M. M.; Brewer, K. J. *Anal. Chem.* **2002**, *74*, 3157−3159.

(8) Anderson, J. D.; McDonald, E. M.; Lee, P. A.; Anderson, M. L.; Ritchie, E. L.; Hall, H. K.; Hopkins, T.; Mash, E. A.; Wang, J.; Padias, A.; Thayumanavan, S.; Barlow, S.; Marder, S. R.; Jabbour, G. E.; Shaheen, S.; Kippelen, B.; Peyghambarian, N.; Wightman, R. M.; Armstrong, N. R. *J. Am. Chem. Soc.* **1998**, *120*, 9646−9655.

(9) Gross, E. M.; Anderson, J. D.; Slaterbeck, A. F.; Thayumanavan, S.; Barlow, S.; Zhang, Y.; Marder, S. R.; Hall, H. K.; Nabor, M. F.; Wang, J. F.; Mash, E. A.; Armstrong, N. R.; Wightman, R. M. *J. Am. Chem. Soc.* **2000**, *122*, 4972−4979.

(10) Kulmala, S.; Håkansson, M.; Spehar, A. M.; Nyman, A.; Kankare, J.; Loikas, K.; Ala-Kleme, T.; Eskola, J. *Anal. Chim. Acta* **2002**, *458*, 271−280.

(11) Gross, E. M.; Armstrong, N. R.; Wightman, R. M. *J. Electrochem. Soc.* **2002**, *149*, E137−E142.

(12) Bruce, D.; Richter, M. M. *Anal. Chem.* **2002**, *74*, 1340−1342.

(13) Kapturkiewicz, A.; Angulu, G. *Dalton Trans.* **2003**, 3907−3913.

(14) Muegge, B. D.; Richter, M. M. *Anal. Chem.* **2004**, *76*, 73−77.

(15) Kim, J. I.; Shin, I.-S.; Kim, H.; Lee, J.-K. *J. Am. Chem. Soc.* **2005**, *127*, 1614−1615.

DOI: 10.1021/ic502444k
Inorg. Chem. 2015, 54, 1446−1453

(16) Li, M. J.; Jiao, P.; Lin, M.; He, W.; Chen, G. N.; Chen, X. *Analyst* **2011**, *136*, 205−210.
(17) Li, C.; Lin, J.; Guo, Y.; Zhang, S. *Chem. Commun.* **2011**, *47*, 4442−4444.
(18) Zhang, S.; Hosaka, M.; Yoshihara, T.; Negishi, K.; Iida, Y.; Tobita, S.; Takeuchi, T. *Cancer Res.* **2010**, *70*, 4490−4498.
(19) Zhou, Y.; Jia, J.; Li, W.; Fei, H.; Zhou, M. *Chem. Commun.* **2013**, *49*, 3230−3232.
(20) Kapturkiewicz, A.; Chen, T.-M.; Laskar, I. R.; Nowacki, J. *Electrochem. Commun.* **2004**, *6*, 827−831.
(21) Swanick, K. N.; Ladouceur, S.; Zysman-Colman, E.; Ding, Z. *Chem. Commun.* **2012**, *48*, 3179−3181.
(22) Yu, L.; Huang, Z.; Liu, Y.; Zhou, M. *J. Organomet. Chem.* **2012**, *718*, 14−21.
(23) Stringer, B. D.; Quan, L. M.; Barnard, P. J.; Wilson, D. J. D.; Hogan, C. F. *Organometallics* **2014**, *33*, 4860−4872.
(24) Yang, W.; Wang, D.; Song, Q.; Zhang, S.; Wang, Q.; Ding, Y. *Organometallics* **2013**, *32*, 4130−4135.
(25) Swanick, K. N.; Ladouceur, S.; Zysman-Colman, E.; Ding, Z. *RSC Adv.* **2013**, *3*, 19961−19964.
(26) Barbante, G. J.; Doeven, E. H.; Kerr, E.; Connell, T. U.; Donnelly, P. S.; White, J. M.; Lópes, T.; Laird, S.; Wilson, D. J. D.; Barnard, P. J.; Hogan, C. F.; Francis, P. S. *Chem.—Eur. J.* **2014**, *20*, 3322−3332.
(27) Zhu, S.; Song, Q.; Zhang, S.; Ding, Y. *J. Mol. Struct.* **2013**, *1035*, 224−230.
(28) Doeven, E. H.; Zammit, E. M.; Barbante, G. J.; Francis, P. S.; Barnett, N. W.; Hogan, C. F. *Chem. Sci.* **2013**, *4*, 977−982.
(29) Zhou, Y.; Li, W.; Liu, Y.; Zeng, L.; Su, W.; Zhou, M. *Dalton Trans.* **2012**, *41*, 9373−9381.
(30) Lamansky, S.; Djurovich, P.; Murphy, D.; Abdel-Razzaq, F.; Lee, H.-E.; Adachi, C.; Burrows, P. E.; Forrest, S. R.; Thompson, M. E. *J. Am. Chem. Soc.* **2001**, *123*, 4304−4312.
(31) Kapturkiewicz, A.; Nowacki, J.; Borowicz, P. *Electrochim. Acta* **2005**, *50*, 3395−3400.
(32) Zhang, G.; Lu, J.; Sabat, M.; Fraser, C. L. *J. Am. Chem. Soc.* **2010**, *132*, 2160−2162.
(33) Krishna, G. R.; Kiran, M. S. R. N.; Fraser, C. L.; Ramamurty, U.; Reddy, C. M. *Adv. Funct. Mater.* **2013**, *23*, 1422−1430.
(34) Song, Y. H.; Chiu, Y. C.; Chi, Y.; Cheng, Y. M.; Lai, C. H.; Chou, P. T.; Wong, K. T.; Tsai, M. H.; Wu, C. C. *Chem.—Eur. J.* **2008**, *14*, 5423−5434.
(35) Hsieh, C. H.; Wu, F. I.; Fan, C. H.; Huang, M. J.; Lu, K. Y.; Chou, P. Y.; Yang, Y. H.; Wu, S. H.; Chen, I. C.; Chou, S. H.; Wong, K. T.; Cheng, C. H. *Chem.—Eur. J.* **2011**, *17*, 9180−9187.
(36) Chang, C. J.; Yang, C. H.; Chen, K.; Chi, Y.; Shu, C. F.; Ho, M. L.; Yeh, Y. S.; Chou, P. T. *Dalton Trans.* **2007**, 1881−1890.
(37) Hung, J. Y.; Chi, Y.; Pai, I. H.; Yu, Y. C.; Lee, G. H.; Chou, P. T.; Wong, K. T.; Chen, C. C.; Wu, C.-C. *Dalton Trans.* **2009**, 6472−6475.
(38) Lin, C. H.; Chi, Y.; Chung, M. W.; Chen, Y. J.; Wang, K. W.; Lee, G. H.; Chou, P. T.; Hung, W. Y.; Chiu, H. C. *Dalton Trans.* **2011**, *40*, 1132−1143.
(39) Li, J.; Djurovich, P. I.; Alleyne, B. D.; Yousufuddin, M.; Ho, N. N.; Thomas, J. C.; Peters, J. C.; Bau, R.; Thompson, M. E. *Inorg. Chem.* **2005**, *44*, 1713−1727.
(40) Sajoto, T.; Djurovich, P. I.; Tamayo, A.; Yousufuddin, M.; Bau, R.; Thompson, M. E.; Holmes, R. J.; Forrest, S. R. *Inorg. Chem.* **2005**, *44*, 7992−8003.
(41) You, Y.; Park, S. Y. *J. Am. Chem. Soc.* **2005**, *127*, 12438−12439.
(42) King, K. A.; Spellane, P. J.; Watts, R. J. *J. Am. Chem. Soc.* **1985**, *107*, 1431−1432.
(43) Runge, E.; Gross, E. K. U. *Phys. Rev. Lett.* **1984**, *52*, 997−1000.
(44) Becke, A. D. *Phys. Rev. A* **1988**, *38*, 3098−3100.
(45) Becke, A. D. *J. Chem. Phys.* **1993**, *98*, 5648−5652.
(46) Perdew, J. P. *Phys. Rev. B* **1986**, *33*, 8822−8824.
(47) McLean, A. D.; Chandler, G. S. *J. Chem. Phys.* **1980**, *72*, 5639−5648.
(48) Hay, P. J.; Wadt, W. R. *J. Chem. Phys.* **1985**, *82*, 270−283.
(49) Hay, P. J.; Wadt, W. R. *J. Chem. Phys.* **1985**, *82*, 299−310.
(50) Shi, L.; Su, J.; Wu, Z. *Inorg. Chem.* **2011**, *50*, 5477−5484.
(51) Shi, L.; Hong, B.; Guan, W.; Wu, Z.; Su, Z. *J. Phys. Chem. A* **2010**, *114*, 6559−6564.
(52) Li, X. N.; Wu, Z. J.; Si, Z. J.; Zhang, H. J.; Zhou, L.; Liu, X. J. *Inorg. Chem.* **2009**, *48*, 7740−7749.
(53) Zhou, M.; Robertson, G. P.; Roovers, J. *Inorg. Chem.* **2005**, *44*, 8317−8325.
(54) Chang, M.-M.; Saji, T.; Bard, A. J. *J. Am. Chem. Soc.* **1977**, *99*, 5399−5403.
(55) Kanoufi, F.; Zu, Y.; Bard, A. J. *J. Phys. Chem. B* **2001**, *105*, 210−216.
(56) Miao, W.; Choi, J.-P.; Bard, A. J. *J. Am. Chem. Soc.* **2002**, *124*, 14478−14485.
(57) Shin, I.-S.; Kim, J. I.; Kwon, T.-H.; Hong, J.-I.; Lee, J.-K.; Kim, H. *J. Phys. Chem. C* **2007**, *111*, 2280−2286.
(58) Frisch, M. J.; Trucks, G. W.; Schlegel, H. B.; Scuseria, G. E.; Robb, M. A.; Cheeseman, J. R.; Montgomery, J. A., Jr.; Vreven, T.; Kudin, K. N.; Burant, J. C.; Millam, J. M.; Iyengar, S. S.; Tomasi, J.; Barone, V.; Mennucci, B.; Cossi, M.; Scalmani, G.; Rega, N.; Petersson, G. A.; Nakatsuji, H.; Hada, M.; Ehara, M.; Toyota, K.; Fukuda, R.; Hasegawa, J.; Ishida, M.; Nakajima, T.; Honda, Y.; Kitao, O.; Nakai, H.; Klene, M.; Li, X.; Knox, J. E.; Hratchian, H. P.; Cross, J. B.; Bakken, V.; Adamo, C.; Jaramillo, J.; Gomperts, R.; Stratmann, R. E.; Yazyev, O.; Austin, A. J.; Cammi, R.; Pomelli, C.; Ochterski, J. W.; Ayala, P. Y.; Morokuma, K.; Voth, G. A.; Salvador, P.; Dannenberg, J. J.; Zakrzewski, V. G.; Dapprich, S.; Daniels, A. D.; Strain, M. C.; Farkas, O.; Malick, D. K.; Rabuck, A. D.; Raghavachari, K.; Foresman, J. B.; Ortiz, J. V.; Cui, Q.; Baboul, A. G.; Clifford, S.; Cioslowski, J.; Stefanov, B. B.; Liu, G.; Liashenko, A.; Piskorz, P.; Komaromi, I.; Martin, R. L.; Fox, D. J.; Keith, T.; Al-Laham, M. A.; Peng, C. Y.; Nanayakkara, A.; Challacombe, M.; Gill, P. M. W.; Johnson, B.; Chen, W.; Wong, M. W.; Gonzalez, C.; Pople, J. A.. *Gaussian 03, Reversion B.02;* Gaussian, Inc.: Wallingford, CT, 2004

DOI: 10.1021/ic502444k
Inorg. Chem. 2015, 54, 1446−1453